

Sensing force gradients with cavity optomechanics while evading backaction

Elisabet K. Arvidsson,¹ Ermes Scarano,¹ August K. Roos,¹ Sofia Qvarfort,^{2,3} and David B. Haviland^{1,*}

¹*Department of Applied Physics, KTH Royal Institute of Technology,
Hannes Alfvéns väg 12, SE-114 19 Stockholm, Sweden*

²*Nordita, KTH Royal Institute of Technology and Stockholm University,
Hannes Alfvéns väg 12, SE-114 19 Stockholm, Sweden*

³*Department of Physics, Stockholm University, AlbaNova University Center, SE-106 91 Stockholm, Sweden*

(Dated: May 10, 2024)

We study force gradient sensing by a coherently driven mechanical resonator with phase-sensitive detection of motion via the two-tone backaction evading measurement of cavity optomechanics. The response of the cavity to two coherent pumps is solved by numerical integration of the classical equations of motion, showing an extended region of monotonic response. We use Floquet theory to model the fluctuations, which rise only slightly above that of the usual backaction evading measurement in the presence of the mechanical drive. Our analysis indicates that this sensing technique is advantageous for applications such as Atomic Force Microscopy.

I. INTRODUCTION

Cavity optomechanical systems have proved to be a good platform for sensing force [1, 2]. Their versatility in size, mechanical frequency and variety of optomechanical interaction has lead to their use in a wide range of applications, from gravitational wave detection [3], to micrometer scale accelerometers [4]. Sensing force gradients with a driven mechanical oscillation is in most cases superior to sensing force via quasi-static displacement of the test mass. A high quality factor mechanical resonator that is coherently driven on resonance experiences a large change in phase for a small change in the force gradient [5, 6]. Furthermore, the coherently driven oscillation allows for lockin detection of displacement, which greatly improves signal to noise ratio.

Cavity optomechanics has achieved remarkable sensitivity, however, no matter how well the measurements are performed, they will inevitably have uncertainty from fluctuations, i.e. noise. Two competing sources of noise, imprecision noise (shot noise) and backaction noise, are minimized at the so-called standard quantum limit (SQL), where each noise source adds an equivalent of a quarter of a phonon of noise energy. [7]. There are techniques to avoid backaction noise, so-called backaction evasion or quantum non-demolition measurements, where the measured observable is a constant of the motion [8]. These techniques have lead to squeezing of mechanical motion below the zero point fluctuation [9]. Other techniques have demonstrated improved sensitivity by exploiting quantum correlations [10] and parametric amplification [11]. Building on backaction evasion, phase-sensitive detection of mechanical motion has been demonstrated with a coherently driven mechanical mode [12, 13].

In this work we investigate the theoretical sensitivity of force gradient detection with a backaction-evasive mea-

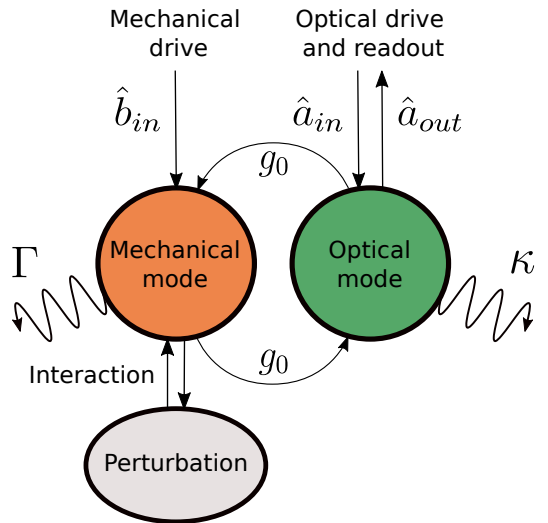


FIG. 1. Schematic of a optical mode with coupling g_0 to a mechanical mode perturbed by an external interaction, e.g. the tip-surface force in AFM. Both modes are driven and experience dissipation. The mechanical mode via \hat{b}_{in} and Γ , and the optical mode via \hat{a}_{in} and κ . Mechanical displacement is read out via the optical mode through \hat{a}_{out} .

surement of a coherently driven mechanical mode. Our work is motivated by the goal of improving dynamic-mode atomic force microscopy (AFM) using a general measurement scheme schematically described in Figure 1. The paper is structured as follows: In section II we describe the system and Hamiltonian. Section III describes the pumping scheme and the classical and quantum dynamics. In Section IV we present the classical response and noise analysis. Finally we summarize and conclude in Section V.

II. MODEL

Standard cavity optomechanics couples a high-frequency electromagnetic mode with resonance fre-

* haviland@kth.se

quency ω_c , to a mechanical mode with resonance frequency ω_m . We use the term 'optical' to refer to the high-frequency mode, which may be microwave or radio frequency. The coupling results in the modulation of ω_c through mechanical displacement x , described by

$$\omega_c(x) \approx \omega_c + \frac{\partial \omega_c}{\partial x} x + \dots \quad (1)$$

where the higher order terms can be neglected if the modulation is small. The total Hamiltonian is

$$\hat{H} = \hbar \omega_c \hat{a}^\dagger \hat{a} + \frac{\hat{p}^2}{2m} + \frac{1}{2} m_{\text{eff}} \omega_m^2 \hat{x}^2 - \frac{\hbar g_0}{x_{\text{zpf}}} \hat{a}^\dagger \hat{a} \hat{x}, \quad (2)$$

where m_{eff} is the effective mass, $x_{\text{zpf}} = \sqrt{\hbar/(2m_{\text{eff}}\omega_m)}$ the zero point fluctuation of the mechanical mode, and $g_0 = -x_{\text{zpf}} \partial \omega_c / \partial x$ the single-photon optomechanical coupling rate. The operators \hat{a} and \hat{a}^\dagger are the annihilation and creation operators of the optical field, obeying the canonical commutator relation $[\hat{a}, \hat{a}^\dagger] = 1$. The mechanical position $\hat{x} = x_{\text{zpf}}(\hat{b} + \hat{b}^\dagger)$ and momentum $\hat{p} = -im_{\text{eff}}\omega_m x_{\text{zpf}}(\hat{b} - \hat{b}^\dagger)$ operators obey $[\hat{x}, \hat{p}] = i\hbar$.

We consider the example of non-contact atomic force microscopy where the mechanical resonator is a cantilever beam, clamped at one end and having a sharp tip at its free end. The tip undergoes small oscillations $x(t)$ about its equilibrium position. The AFM scanner controls the distance h between this equilibrium position and the surface. When the tip is close to the surface it experiences an interaction approximated by a van der Waals potential between a sphere and a flat surface,

$$U(x) = -\frac{HR_{\text{tip}}}{6(h+x)} \quad (3)$$

where H is the Hamaker constant and R_{tip} radius of the tip [14]. For small deviation x , we Taylor expand the potential, truncating after the second order. Promoting x to an operator gives,

$$U(\hat{x}) = -\frac{HR_{\text{tip}}}{6h} \left(1 - \frac{\hat{x}}{h} + \frac{\hat{x}^2}{h^2} \right) + \mathcal{O}(\hat{x}^3). \quad (4)$$

The first term is simply a static shift which will not impact the equations of motion and can be disregarded.

The Hamiltonian with the truncated tip-surface force included reads as follows

$$\hat{H} = \hbar \omega_c \hat{a}^\dagger \hat{a} + \frac{\hat{p}^2}{2m} + \frac{1}{2} m \omega_m^2 \hat{x}^2 - \frac{\hbar g_0}{x_{\text{zpf}}} \hat{a}^\dagger \hat{a} \hat{x} - F_1 \hat{x} - F_2 \hat{x}^2 \quad (5)$$

where $F_1 = -HR_{\text{tip}}/(6h^2)$ is a static tip-surface force which moves the equilibrium position of the mechanical mode. The force gradient $F_2 = HR_{\text{tip}}/(6h^3)$ results in an effective shift of the mechanical resonance frequency,

$$\omega_{\text{eff}} = \sqrt{\omega_m^2 - 2F_2/m_{\text{eff}}}. \quad (6)$$

Rewriting the Hamiltonian with the effective resonance frequency,

$$\hat{H} = \hbar \omega_c \hat{a}^\dagger \hat{a} + \frac{\hat{p}^2}{2m} + \frac{1}{2} m \omega_{\text{eff}}^2 (F_2) \hat{x}^2 - \frac{\hbar g_0}{x_{\text{zpf}}} \hat{a}^\dagger \hat{a} \hat{x} - F_1 \hat{x} \quad (7)$$

we transform into a frame rotating with respect to an optical frequency which is detuned from cavity resonance $\omega_p = \omega_c + \Delta$. In terms of mechanical annihilation and creation operators the Hamiltonian reads,

$$\hat{H}_{\text{rot}} = -\hbar \Delta \hat{a}^\dagger \hat{a} + \hbar \omega_{\text{eff}} (F_2) \hat{b}^\dagger \hat{b} - \hbar g_0 \hat{a}^\dagger \hat{a} (\hat{b} + \hat{b}^\dagger) - F_1 x_{\text{zpf}} (\hat{b} + \hat{b}^\dagger). \quad (8)$$

Note that the coupling g_0 depends on the mechanical resonance frequency through x_{zpf} , but here we treat it as a constant, considering only small changes of ω_m .

III. FORCE GRADIENT SENSING

A. Optical pumps and mechanical drive

We consider the case where the mechanical mode is coherently driven at a frequency ω_d which is close to ω_{eff} . The cavity is pumped with two tones $\omega_{\pm} = \omega_p \pm \omega_d$, detuned from the optical pumps center frequency ω_p by ω_d . The resulting sidebands from the optomechanical interaction interfere at ω_p where the amplitude of the response depends on the phase of the mechanical motion. The phase of the mechanical oscillator is thus detected in relation to the phase of the beating envelope realized by the two optical pumps. We allow for a slight detuning Δ of ω_p from the cavity resonance: $\omega_p = \omega_c + \Delta$. The optical input field reads

$$\hat{a}_{\text{in}} = \bar{a}_{\text{in}-} e^{-i\omega_d t} + \bar{a}_{\text{in}+} e^{-i\omega_d t} + \hat{d}_{\text{in}} \quad (9)$$

where the first two terms are the classical pump signals, and \hat{d}_{in} accounts for any input fluctuations. In a backaction evading measurement the pumps should be placed with no detunings such that $\omega_p = \omega_c$ and $\omega_d = \omega_{\text{eff}}$ leading to $\omega_{\pm} = \omega_c \pm \omega_{\text{eff}}$, as any detuning induces backaction into the measurement.

The mechanical mode is driven by a single tone close to its effective resonance frequency, $\omega_d = \omega_{\text{eff}} + \delta$ where δ is a small detuning. The mechanical drive reads

$$\hat{b}_{\text{in}} = \bar{\beta}_{\text{in}} e^{-i\omega_d t} + \hat{c}_{\text{in}} \quad (10)$$

with \hat{c}_{in} accounting for fluctuations. Here all drive terms have complex amplitudes denoted with a bar, representing classical signals, for example $\bar{\beta}_{\text{in}} = |\beta_{\text{in}}| e^{-i\phi_m}$.

B. Quantum and classical dynamics

In the frame rotating with the pump center frequency ω_p , we obtain the following Langevin equations of motion for the optical and mechanical modes,

$$\begin{aligned}\dot{\hat{a}} &= i\Delta\hat{a} + ig_0\hat{a}(\hat{b} + \hat{b}^\dagger) - \frac{\kappa}{2}\hat{a} \\ &\quad - \sqrt{\kappa}(\bar{a}_{in-}e^{i\omega_dt} + \bar{a}_{in+}e^{-i\omega_dt}) - \sqrt{\kappa}\hat{d}_{in} \\ \dot{\hat{b}} &= -i\omega_{eff}(F_2)\hat{b} + ig_0\hat{a}^\dagger\hat{a} + \frac{iF_1x_{zpf}}{\hbar} - \frac{\Gamma}{2}\hat{b} \\ &\quad - \sqrt{\Gamma}|\bar{\beta}_{in}|e^{-i\phi_m}e^{-i\omega_dt} - \sqrt{\Gamma}\hat{c}_{in}\end{aligned}\quad (11)$$

where κ and Γ are the total optical and mechanical dissipation rates, respectively. We make the assumption that the internal cavity losses are small in comparison to the external decay rate, such that $\kappa_{ext} \approx \kappa$. In other words, the force sensor is designed for an over-coupled cavity in which damping is dominated by useful signal flowing to the next stage in the detection chain.

We model the optical and mechanical response as small quantum fluctuations around a mean,

$$\begin{aligned}\hat{a} &= \bar{a} + \hat{d} \\ \hat{b} &= \bar{\beta} + \hat{c},\end{aligned}\quad (12)$$

where the expectation values $\bar{a} = \langle \hat{a} \rangle$ and $\bar{\beta} = \langle \hat{b} \rangle$ correspond to the classical oscillatory motion of the optical and mechanical modes respectively. Inserting Eq. (12) into Eq. (11), we find the Langevin equations for the quantum fluctuations.

$$\begin{aligned}\dot{\hat{d}} &= i\Delta\hat{d} + ig_0(\bar{a} + \hat{d})(\bar{\beta} + \hat{c} + \bar{\beta}^* + \hat{c}^\dagger) - \frac{\kappa}{2}\hat{d} - \sqrt{\kappa}\hat{d}_{in} \\ \dot{\hat{c}} &= -i\omega_{eff}(F_2)\hat{c} + ig_0(\bar{a}^* + \hat{d}^\dagger)(\bar{a} + \hat{d}) - \frac{\Gamma}{2}\hat{c} - \sqrt{\Gamma}\hat{c}_{in}\end{aligned}\quad (13)$$

and the classical motion

$$\begin{aligned}\dot{\bar{a}} &= i\Delta\bar{a} + ig_0\bar{a}(\bar{\beta} + \bar{\beta}^*) - \frac{\kappa}{2}\bar{a} \\ &\quad - \sqrt{\kappa}(\bar{a}_{in-}e^{i\omega_dt} + \bar{a}_{in+}e^{-i\omega_dt}) \\ \dot{\bar{\beta}} &= -i\omega_{eff}(F_2)\bar{\beta} + ig_0|\bar{a}|^2 + \frac{iF_1x_{zpf}}{\hbar} - \frac{\Gamma}{2}\bar{\beta} \\ &\quad - \sqrt{\Gamma}|\bar{\beta}_{in}|e^{-i\phi_m}e^{-i\omega_dt}\end{aligned}\quad (14)$$

In the usual two-tone backaction evading measurement [15] these equations do not include the terms with F_1 , F_2 or $\bar{\beta}_{in}$, and can therefore be solved analytically in the frequency domain. In our case, the introduction of the perturbing force and the mechanical drive leads us to solve the equations numerically.

IV. RESULTS

Solving the classical equations of motions (14) we show how the force gradient F_2 is detected from the cavity field at ω_p . Using (13) we model the noise and compare it to the usual backaction evasion case.

A. Modelling the classical response

We solve the classical equations of motion (14) by numerical integration using the scipy function ODEint [16]. We simulate a tip-surface interaction given in Section II with $HR_{tip} = 3.55 \cdot 10^{-29}$ Jm, for example achieved with $H = 0.03$ aJ and $R_{tip} = 1.183$ nm, with an optical pump amplitude of $\bar{a}_{in\pm} = 1.62271 \cdot 10^5 \sqrt{\text{photons/s}}$, corresponding to the power needed to reach SQL for an optical (microwave) mode with resonance frequency $\omega_c/2\pi = 4.5$ GHz and total decay rate $\kappa/2\pi = 1$ MHz, coupled to a mechanical mode with resonance frequency $\omega_m/2\pi = 5.37$ MHz, total decay rate $\Gamma/2\pi = 2.3$ kHz, effective mass $m_{eff} = 54$ pg, with an optomechanical coupling rate $g_0/2\pi = 1$ kHz. The large mechanical linewidth is chosen to reduce computational time. We apply a mechanical drive to yield an oscillation amplitude corresponding to $200x_{zpf}$. We initially set the scanner position to $h = 0.3$ nm, approaching and retracting from the surface to obtain a mechanical frequency shift of one linewidth $\omega_{eff} \pm \Gamma$. The Fourier transform of the solutions of the mechanical motion and the optical field are plotted in Figure 2 (a) and (b) for a mechanical drive phase $\phi_m = 0.86\pi$ and $\omega_{eff} = \omega_d$. The approximated optical and mechanical fields reads

$$\bar{a}(t) \approx \bar{a}_-e^{i\omega_dt} + \bar{a}_c + \bar{a}_+e^{-i\omega_dt} \quad (15)$$

$$\bar{\beta}(t) \approx \bar{\beta}_0 + \bar{\beta}_1e^{-i\omega_dt} \quad (16)$$

where any contribution less than that of the zero point fluctuations for each respective mode is neglected. The term $\bar{\beta}_0$ is due to the static force which induces a shift in the optical resonance. The term $\bar{\beta}_1$ is the response to the mechanical drive modulating the cavity resonance. In the following analysis $2g_0|\bar{\beta}_1| \ll \kappa$ so that the linearization in Eq. 1 is valid [17].

The quantity of interest is the term \bar{a}_c describing the coherent optical response at frequency ω_p , which is a superposition of the upper mechanical sideband from the red pump, and the lower mechanical sideband from the blue pump. The magnitude of \bar{a}_c depends on the phase of the mechanical mode in relation to the phase of the beat created by the two optical pumps. We change the phase of the mechanical mode either through the mechanical drive phase ϕ_m , or by changing effective mechanical resonance frequency through the force gradient $\omega_{eff}(F_2)$.

In Fig. 2(b) we plot the change in magnitude $\Delta\bar{a}_c = \bar{a}_c - \bar{a}_{c,stop}$ versus ϕ_m and ω_{eff} where $\bar{a}_{c,stop}$ is a setpoint for the AFM scanning feedback that controls h . A cut along the vertical dash-dotted line reveals the interference between the two mechanical sidebands, shown in the rightmost panel. The horizontal dashed line represents a typical setpoint for feedback, locking to the mechanical phase in the middle of an interference fringe. We see in the lower panel that the change in response is monotonic with shift of mechanical resonance frequency $|\omega_d - \omega_{eff}| \leq 0.2\Gamma$ (purple shaded area). The extended region of monotonic response to changes in ω_{eff} makes

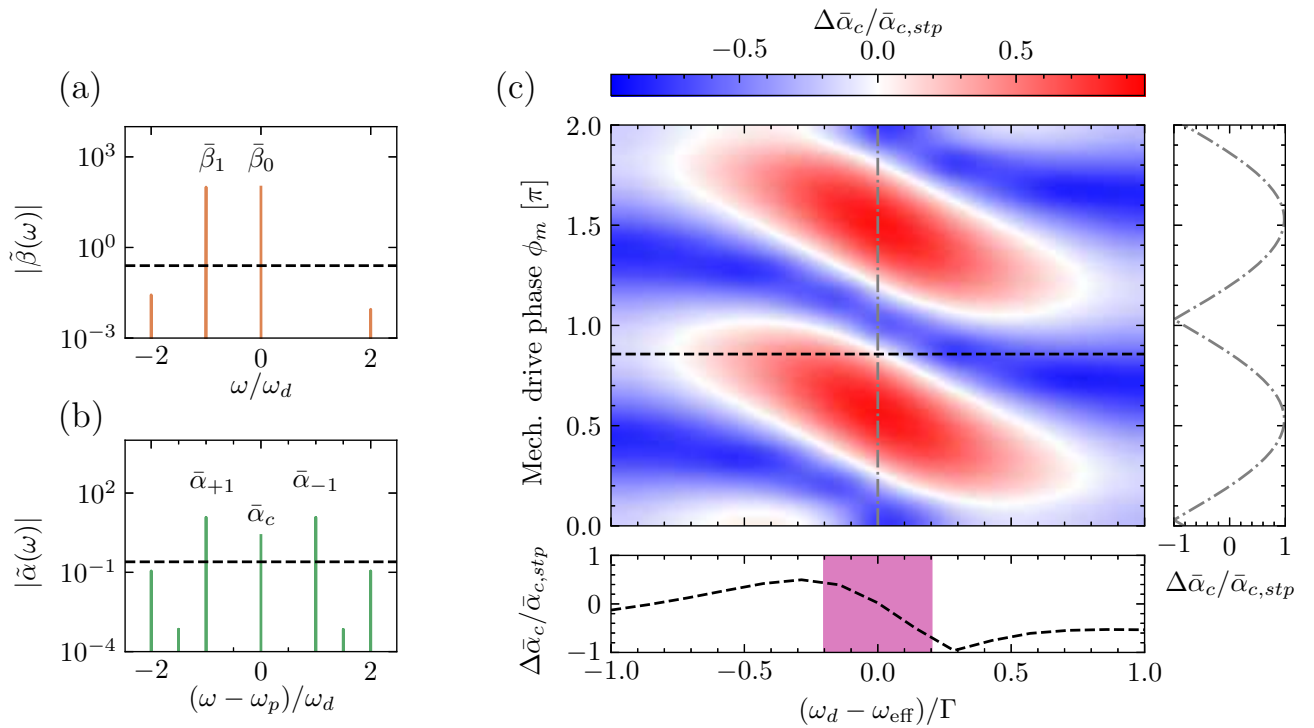


FIG. 2. (a) and (b) Fourier transform of the solutions to the mechanical and optical classical equations of motion where the frequency components included in the following noise analysis are labeled. The black dashed lines indicate the square root of the zero point fluctuations. (c) Change in magnitude of the optical coherent tone $\bar{\alpha}_c$ normalized to a setpoint value $\bar{\alpha}_{c,stp}$ as a function of mechanical drive phase ϕ_m and effective mechanical resonance frequency ω_{eff} . To the right a vertical cut is shown detailing the interference pattern and on the bottom a horizontal cut where the purple region is highlighting the possible region of operation.

$\bar{\alpha}_{c,stp}$ a useful setpoint for scanning feedback.

$$\dot{\hat{c}} = -i\omega_{\text{eff}}(F_2)\hat{c} + ig_0[(\bar{\alpha}_- e^{-i\omega_d t} + \bar{\alpha}_c^* + \bar{\alpha}_+^* e^{i\omega_d t})\hat{d} + (\bar{\alpha}_- e^{i\omega_d t} + \bar{\alpha}_c + \bar{\alpha}_+ e^{-i\omega_d t})\hat{d}^\dagger] - \frac{\Gamma}{2}\hat{c} - \sqrt{\Gamma}\hat{c}_{\text{in}} \quad (18)$$

B. Noise analysis

In the usual backaction evading measurement the two-tone pumped optical cavity detects one of the mechanical quadratures without adding fluctuations to that quadrature. However, in dynamic AFM where the mechanical mode is coherently driven, the combination of both optical pumping and mechanical driving leads to couplings which channel backaction fluctuations on to the detected quadrature. When examining quantum limits to sensing force gradients, it is important to consider the impact of these additional noise contributions.

Returning to the equations of motions, we insert Eqs. (15) and (16) into Eq. (13) and linearize to obtain

$$\begin{aligned} \dot{\hat{d}} = i\tilde{\Delta}\hat{d} + ig_0[(\bar{\alpha}_- e^{i\omega_d t} + \bar{\alpha}_c + \bar{\alpha}_+ e^{-i\omega_d t})\hat{c} + (\bar{\alpha}_- e^{i\omega_d t} \\ + \bar{\alpha}_c + \bar{\alpha}_+ e^{-i\omega_d t})\hat{c}^\dagger + \hat{d}(\bar{\beta}_1 e^{-i\omega_d t} + \bar{\beta}_1^* e^{i\omega_d t})] \\ - \frac{\kappa}{2}\hat{d} - \sqrt{\kappa}\hat{d}_{\text{in}} \end{aligned} \quad (17)$$

where $\tilde{\Delta} = \Delta + g_0(\bar{\beta}_0 + \bar{\beta}_0^*)$. At the setpoint of operation the placement of the pump center frequency can be adjusted such that $\tilde{\Delta} = 0$. As the AFM scanner moves and the static displacement $\bar{\beta}_0$ changes, a small non-zero detuning $\tilde{\Delta}$ needs to be taken into account. We see that both the optical (Eq. 17) and mechanical (Eq. 18) fluctuations are periodic with ω_d , complicating the analysis. To solve for these fluctuations we turn to Floquet theory using the same approach as in [18, 19] where we expand according to

$$\hat{d}(t) = \sum_{n=-\infty}^{\infty} e^{in\omega_d t} \hat{d}^{(n)}(t), \quad \hat{d}^\dagger(t) = \sum_{n=-\infty}^{\infty} e^{in\omega_d t} \hat{d}^{(n)\dagger}(t). \quad (19)$$

where $\hat{d}^{(n)}$ denotes a Fourier operator (in either time or frequency domain) rotating at frequency $n\omega_d$. Rewriting Eqs. (17) and (18) in the form of stationary Langevin equations of motion and Fourier transforming the equa-

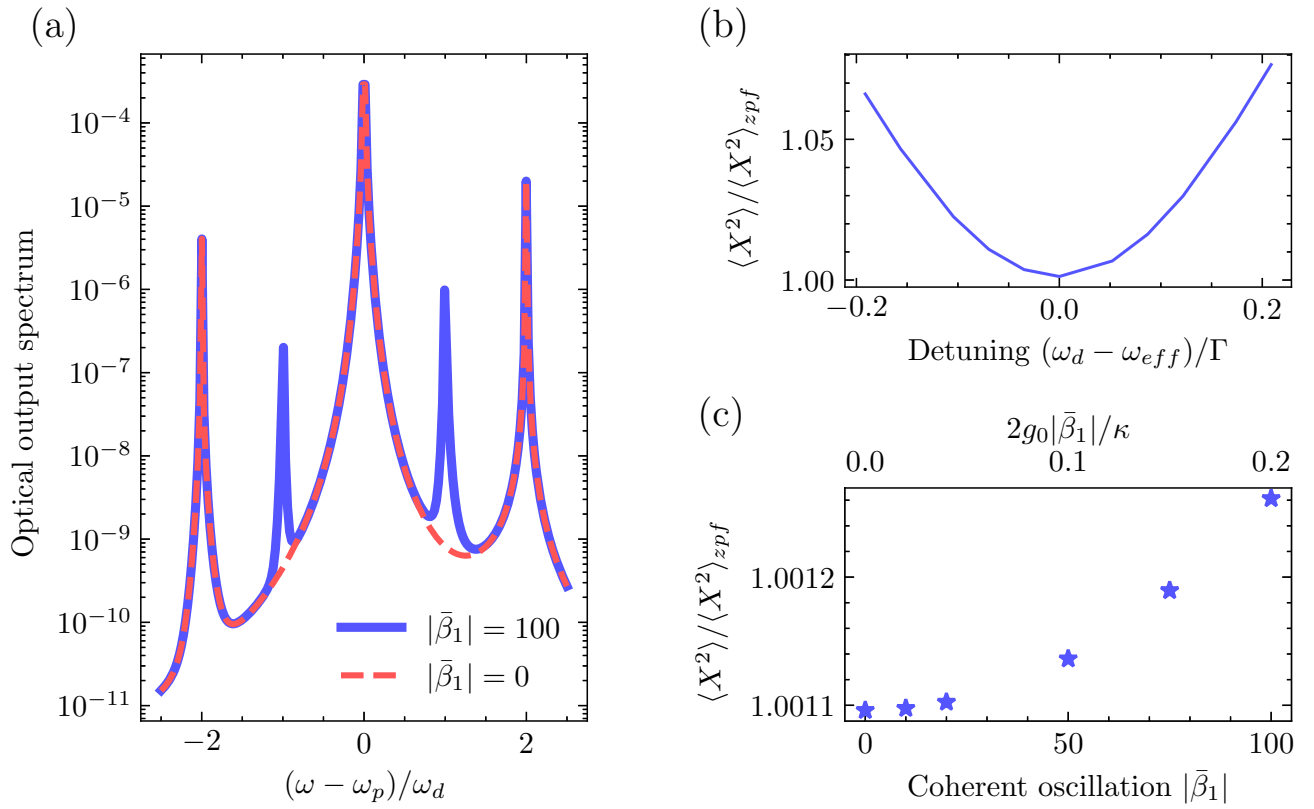


FIG. 3. (a) Optical output spectrum detailing the difference between the pure backaction evasion with no mechanical drive $|\bar{\beta}_1| = 0$, and force gradient sensing with a mechanical drive $|\bar{\beta}_1| = 100$. The addition of a coherent drive does not significantly add noise. (b) Quadrature fluctuations of the mechanical mode as a function of the detuning, calculated for $|\bar{\beta}_1| = 100$. The range of detuning is chosen to match the monotonic regime of the classical response. (c) Quadrature fluctuations normalized to the zero point fluctuation plotted against $|\bar{\beta}_1|$ for the case of resonant drive ($\omega_d = \omega_{eff}$).

tions gives

$$\begin{aligned} -i\omega\hat{d}^{(n)} &= (i\tilde{\Delta} - i\omega_d)\hat{d}^{(n)} + ig_0(\bar{\alpha}_-\hat{x}^{(n-1)} + \bar{\alpha}_+\hat{x}^{(n+1)}) \\ &\quad + ig_0\bar{\alpha}_c\hat{x}^{(n)} + ig_0(\bar{\beta}_1\hat{d}^{(n+1)} + \bar{\beta}_1^*\hat{d}^{(n-1)}) \\ &\quad - \frac{\kappa}{2}\hat{d}^{(n)} - \sqrt{\kappa}d_{in}^{(n)} \end{aligned} \quad (20)$$

$$\begin{aligned} -i\omega\hat{c}^{(n)} &= -i[\omega_{eff}(F_2) + n\omega_d]\hat{c}^{(n)} + ig_0(\bar{\alpha}_-\hat{d}^{(n-1)\dagger} \\ &\quad + \bar{\alpha}_+\hat{d}^{(n+1)\dagger}) + ig_0(\bar{\alpha}_-\hat{d}^{(n+1)} + \bar{\alpha}_+\hat{d}^{(n-1)}) \\ &\quad + ig_0(\bar{\alpha}_c^*\hat{d}^{(n)} + \bar{\alpha}_c\hat{d}^{(n)\dagger}) - \frac{\Gamma}{2}\hat{c}^{(n)} - \sqrt{\Gamma}\hat{c}_{in}^{(n)} \end{aligned} \quad (21)$$

where $\hat{x}^{(n)} = \hat{c}^{(n)} + \hat{c}^{(n)\dagger}$. For the full calculation see Appendix A.

To understand how the mechanical drive and force gradient impacts fluctuations, we first calculate the fluctuations of the mechanical mode and later the spectrum of the output optical field.

We define the mechanical quadrature rotating at frequency ω_d , coupled to the optical field in the back action evading measurement [1] as

$$\hat{X} = \frac{1}{\sqrt{2}}(\hat{c}e^{i\omega_d t} + \hat{c}^\dagger e^{-i\omega_d t}). \quad (22)$$

The variance of this quadrature is (see Appendix C)

$$\begin{aligned} \langle \hat{X}^2 \rangle &= \int \frac{d\omega}{2\pi} S_{XX}^{(0)}(\omega) = \frac{1}{2} \int \frac{d\omega}{2\pi} [S_{cc}^{(-2)}(\omega + \omega_d) \\ &\quad + S_{cc^\dagger}^{(0)}(\omega + \omega_d) + S_{c^\dagger c^\dagger}^{(2)}(\omega - \omega_d) + S_{c^\dagger c}^{(0)}(\omega - \omega_d)] \end{aligned} \quad (23)$$

where the power spectrum is defined as

$$S_{OO'}^{(m)}(\omega) = \sum_n \int \frac{d\omega'}{2\pi} \langle \hat{O}^{(n)}(\omega + n\omega_d) \hat{O}'^{(m-n)}(\omega') \rangle. \quad (24)$$

To calculate the optical spectrum we first write the equations for the terms at $n \pm 1$

$$\begin{aligned} \hat{d}^{(n+1)} &= ig_0\chi_c(\omega - \omega_d(n+1))(\bar{\alpha}_-\hat{x}^{(n)} + \bar{\alpha}_+\hat{x}^{(n+2)} \\ &\quad + \bar{\alpha}_c\hat{x}^{(n+1)} + \bar{\beta}_1\hat{d}^{(n+2)} + \bar{\beta}_1^*\hat{d}^{(n)}) \\ \hat{d}^{(n-1)} &= ig_0\chi_c(\omega - \omega_d(n-1))(\bar{\alpha}_-\hat{x}^{(n-2)} + \bar{\alpha}_+\hat{x}^{(n)} \\ &\quad + \bar{\alpha}_c\hat{x}^{(n-1)} + \bar{\beta}_1\hat{d}^{(n)} + \bar{\beta}_1^*\hat{d}^{(n-2)}) \end{aligned} \quad (25)$$

where we have introduced the optical susceptibility $\chi_c(\omega) = [\kappa/2 - i(\omega + \tilde{\Delta})]^{-1}$. Discarding the terms at $n \pm 2$, valid for fast periodic modulation $\omega_d \gg \kappa, \Gamma$ [20],

we use Eq. (25) to arrive at an expression for the Fourier operators of the optical mode

$$\hat{d}^{(n)} = \chi'_c(\omega) i g_0 (\bar{\alpha}'_- x^{(n-1)} + \bar{\alpha}'_+ x^{(n+1)} + \bar{\alpha}'_c x^{(n)}) \quad (26)$$

where the modified optical susceptibility is

$$\chi'_c(\omega) = [\chi_c(\omega - \omega_d n)^{-1} + g_0^2 |\bar{\beta}_1|^2 \chi_c(\omega - \omega_d(n+1)) + g_0^2 |\bar{\beta}_1|^2 \chi_c(\omega - \omega_d(n-1))]^{-1} \quad (27)$$

and where we have defined

$$\bar{\alpha}'_- = \bar{\alpha}_- + i g_0 \bar{\beta}_1^* \chi_c(\omega - \omega_d(n-1)) \bar{\alpha}_c \quad (28)$$

$$\bar{\alpha}'_+ = \bar{\alpha}_+ + i g_0 \bar{\beta}_1 \chi_c(\omega - \omega_d(n+1)) \bar{\alpha}_c \quad (29)$$

$$\begin{aligned} \bar{\alpha}'_c &= \bar{\alpha}_c + i g_0 \bar{\beta}_1 \chi_c(\omega - \omega_d(n+1)) \bar{\alpha}_- \\ &\quad + i g_0 \bar{\beta}_1^* \chi_c(\omega - \omega_d(n-1)) \bar{\alpha}_+ \end{aligned} \quad (30)$$

The measured power spectral density is given by the $m = 0$ component [18] of Eq. 24 (see Appendix B)

$$\begin{aligned} S_{d^\dagger d}^{(0)}(\omega) &= |\chi'_c(\omega)|^2 g_0^2 [|\bar{\alpha}'_-|^2 S_{xx}^{(0)}(\omega + \omega_d) \\ &\quad + |\bar{\alpha}'_+|^2 S_{xx}^{(0)}(\omega - \omega_d) + \bar{\alpha}'_-^* \bar{\alpha}'_+ S_{xx}^{(-2)}(\omega + \omega_d) \\ &\quad + \bar{\alpha}'_+^* \bar{\alpha}'_- S_{xx}^{(2)}(\omega - \omega_d) + |\bar{\alpha}'_c|^2 S_{xx}^{(0)}(\omega) \\ &\quad + \bar{\alpha}'_-^* \bar{\alpha}'_c S_{xx}^{(-1)}(\omega + \omega_d) + \bar{\alpha}'_+^* \bar{\alpha}'_c S_{xx}^{(1)}(\omega - \omega_d) \\ &\quad + \bar{\alpha}'_c^* \bar{\alpha}'_- S_{xx}^{(1)}(\omega) + \bar{\alpha}'_c^* \bar{\alpha}'_+ S_{xx}^{(-1)}(\omega)] \end{aligned} \quad (31)$$

If $\bar{\alpha}_- = \bar{\alpha}_+$ the first four terms in Eqs. (31) constitute the standard backaction evasion spectrum, where we have not used the rotating wave approximation.

Figure 3(a) shows a comparison of the optical output power spectral density $S_{d_{out}^\dagger d_{out}}^{(0)}(\omega) = \kappa S_{d^\dagger d}^{(0)}(\omega)$ for two cases: a coherent mechanical state driven at $\omega_d = \omega_{eff}$ with $|\bar{\beta}_1| = 100$ corresponding to a oscillation magnitude of $200x_{zpf}$, and the usual backaction evading measurement with $|\bar{\beta}_1| = 0$. In both cases the thermal mechanical phonon occupancy $\bar{n}_m^{th} = 0$ and thermal cavity photon occupancy $\bar{n}_c^{th} = 0$. We see that the spectrum in the driven case shows additional noise peaks around the two optical pump frequencies, stemming from the mixing of the coherent optical response $\bar{\alpha}_c$ with the mechanical thermal noise. The peaks at $\pm 2\omega_{eff}$ are due to backaction usually neglected in the rotating wave approximation.

To further see the effect of the mechanical resonance frequency shift from the influence of the tip-surface force gradient, we calculate the variance of the measured mechanical quadrature. The mechanical resonance frequency shift results in an effective detuning of the two optical pumps from the optimal pumping configuration of the backaction evading measurement ($\omega_{\pm} = \omega_c \pm \omega_{eff}$). The effect of this detuning on the quadrature fluctuations has previously been investigated in [21] but without a mechanical drive. Figure 3(b) shows the increase in the variance of the mechanical quadrature due to backaction noise as a function of the effective mechanical resonance frequency. For no detuning the quadrature fluctuation is very close to that of the unmeasured mechanical state.

As the tip-surface force gradient introduces a change in the effective resonance frequency, additional backaction noise is introduced into the quadrature. This leads to an increase of the noise around the center frequency component $\bar{\alpha}_c$ in the output optical field.

Figure 3(c) shows the fluctuations at zero detuning for several coherent oscillation amplitudes $|\bar{\beta}_1|$ of the mechanical mode. We see that the additional backaction noise increases with the amplitude of the mechanical motion, however, the increase in quadrature fluctuations from the detuning is much larger than that from the mechanical drive. The upper x-axis gives the corresponding values of $2g_0|\bar{\beta}_1|/\kappa \ll 1$ where the linearized optomechanical interaction is valid.

V. SUMMARY AND CONCLUSIONS

We examined a scheme for force gradient sensing with a driven mechanical mode where motion is detected with the two-tone backaction evading measurement of cavity optomechanics. We envision this technique being useful in for example low temperature atomic force microscopy but also for other types of force gradient detection. The detection principle gives a monotonic response to changes in force gradient which cause frequency shifts on the order of 20% of the mechanical linewidth. A smaller mechanical linewidth improves the force sensitivity, but limits the region of monotonic response for feedback control of Atomic Force Microscopy.

Using Floquet theory to analyze the equations of motion of fluctuating terms, we showed that quadrature fluctuations of the mechanical mode, as detected in the optical output spectrum, are only slightly larger than that achieved with the usual backaction evading measurement (see Fig. 3(b) and (c)). The majority of the increase in fluctuations comes from the change of the effective mechanical resonance due to the force gradient, resulting in a detuning of the optical pumps from the optimal placement for backaction evasion. The contribution of the mechanical drive to the increase in fluctuations is much less than that of the change of the mechanical resonance frequency.

To further decrease the noise of the mechanical quadrature and the noise around the center pump frequency, one can adjust the amplitudes of the two optical pumps such that $|\bar{\alpha}_{in-}| > |\bar{\alpha}_{in+}|$ to produce a squeezed mechanical state. For a mechanical resonator close to its ground state, this squeezing can result in a quadrature fluctuation less than the zero point fluctuations. However, un-equal pump amplitudes changes the region of monotonic response in the classical interference pattern, as complete destructive and constructive interference is no longer achieved.

ACKNOWLEDGEMENTS

The authors would like to thank Clara Wanjura as well as the QAFM team for fruitful discussions: T. Glatzel, M. Zutter, E. Tholén, D. Forchheimer, I. Ignat, M. Kwon, and D. Platz. E.K.A., E.S., A.K.R., are supported by an EIC Pathfinder (FET Open) grant 828966 – QAFM and the Swedish SSF grant ITM17-0343. S.Q. is funded in part by the Wallenberg Initiative on Networks and Quantum Information (WINQ) and in part by the Marie Skłodowska-Curie Action IF programme *Nonlin-*

ear optomechanics for verification, utility, and sensing (NOVUS) – Grant-Number 101027183. Nordita is supported in part by NordForsk.

DATA AVAILABILITY

The data that support the findings of this study are openly available in Zenodo at <https://doi.org/10.5281/zenodo.11175476>, reference number 11175476.

[1] Markus Aspelmeyer, Tobias J. Kippenberg, and Florian Marquardt. Cavity optomechanics. *Rev. Mod. Phys.*, 86: 1391–1452, Dec 2014. doi:10.1103/RevModPhys.86.1391. URL <https://link.aps.org/doi/10.1103/RevModPhys.86.1391>.

[2] Bei-Bei Li, Lingfeng Ou, Yuechen Lei, and Yong-Chun Liu. Cavity optomechanical sensing. *Nanophotonics*, 10(11):2799–2832, 2021. doi:doi:10.1515/nanoph-2021-0256. URL <https://doi.org/10.1515/nanoph-2021-0256>.

[3] B. P. Abbott et al. Observation of gravitational waves from a binary black hole merger. *Phys. Rev. Lett.*, 116: 061102, Feb 2016. doi:10.1103/PhysRevLett.116.061102. URL <https://link.aps.org/doi/10.1103/PhysRevLett.116.061102>.

[4] Alexander G. Krause, Martin Winger, Tim D. Blasius, Qiang Lin, and Oskar Painter. A high-resolution microchip optomechanical accelerometer. *Nature Photonics*, 6(11):768–772, Nov 2012. ISSN 1749-4893. doi:10.1038/nphoton.2012.245. URL <https://doi.org/10.1038/nphoton.2012.245>.

[5] D. P. E. Smith. Limits of force microscopy. *Review of Scientific Instruments*, 66(5):3191–3195, 05 1995. ISSN 0034-6748. doi:10.1063/1.1145550. URL <https://doi.org/10.1063/1.1145550>.

[6] T. R. Albrecht, P. Grütter, D. Horne, and D. Rugar. Frequency modulation detection using high-Q cantilevers for enhanced force microscope sensitivity. *Journal of Applied Physics*, 69(2):668–673, 01 1991. ISSN 0021-8979. doi:10.1063/1.347347. URL <https://doi.org/10.1063/1.347347>.

[7] A. A. Clerk, M. H. Devoret, S. M. Girvin, Florian Marquardt, and R. J. Schoelkopf. Introduction to quantum noise, measurement, and amplification. *Rev. Mod. Phys.*, 82:1155–1208, Apr 2010. doi:10.1103/RevModPhys.82.1155. URL <https://link.aps.org/doi/10.1103/RevModPhys.82.1155>.

[8] Vladimir B. Braginsky, Yuri I. Vorontsov, and Kip S. Thorne. Quantum nondemolition measurements. *Science*, 209(4456):547–557, Aug 1980. doi:10.1126/science.209.4456.547. URL <https://doi.org/10.1126/science.209.4456.547>.

[9] E. E. Wollman, C. U. Lei, A. J. Weinstein, J. Suh, A. Kronwald, F. Marquardt, A. A. Clerk, and K. C. Schwab. Quantum squeezing of motion in a mechanical resonator. *Science*, 349(6251):952–955, 2015. doi:10.1126/science.aac5138. URL <https://www.science.org/doi/abs/10.1126/science.aac5138>.

[10] David Mason, Junxin Chen, Massimiliano Rossi, Yeghishe Tsaturyan, and Albert Schliesser. Continuous force and displacement measurement below the standard quantum limit. *Nature Physics*, 15(8):745–749, Aug 2019. ISSN 1745-2481. doi:10.1038/s41567-019-0533-5. URL <https://doi.org/10.1038/s41567-019-0533-5>.

[11] Ali Motazedifarid, A. Dalafi, F. Bemani, and M. H. Naderi. Force sensing in hybrid bose-einstein-condensate optomechanics based on parametric amplification. *Phys. Rev. A*, 100:023815, Aug 2019. doi:10.1103/PhysRevA.100.023815. URL <https://link.aps.org/doi/10.1103/PhysRevA.100.023815>.

[12] J. B. Hertzberg, T. Rocheleau, T. Ndukum, M. Savva, A. A. Clerk, and K. C. Schwab. Back-action-evasive measurements of nanomechanical motion. *Nature Physics*, 6(3):213–217, December 2009. doi:10.1038/nphys1479. URL <https://doi.org/10.1038/nphys1479>.

[13] August K. Roos, Ermes Scarano, Elisabet K. Arvidsson, Erik Holmgren, and David B. Haviland. Kinetic inductive electromechanical transduction for nanoscale force sensing. *Phys. Rev. Appl.*, 20:024022, Aug 2023. doi:10.1103/PhysRevApplied.20.024022. URL <https://link.aps.org/doi/10.1103/PhysRevApplied.20.024022>.

[14] Franz J. Giessibl. Advances in atomic force microscopy. *Rev. Mod. Phys.*, 75:949–983, Jul 2003. doi:10.1103/RevModPhys.75.949. URL <https://link.aps.org/doi/10.1103/RevModPhys.75.949>.

[15] W.P. Bowen and G.J. Milburn. *Quantum Optomechanics*. Taylor & Francis, Boca Raton, first edition, 2015. ISBN 9781482259155. URL <https://doi.org/10.1201/b19379>.

[16] Pauli Virtanen, Ralf Gommers, Travis E. Oliphant, Matt Haberland, Tyler Reddy, David Cournapeau, Evgeni Burovski, Pearu Peterson, Warren Weckesser, Jonathan Bright, Stéfan J. van der Walt, Matthew Brett, Joshua Wilson, K. Jarrod Millman, Nikolay Mayorov, Andrew R. J. Nelson, Eric Jones, Robert Kern, Eric Larson, C J Carey, İlhan Polat, Yu Feng, Eric W. Moore, Jake VanderPlas, Denis Laxalde, Josef Perktold, Robert Cimrman, Ian Henriksen, E. A. Quintero, Charles R. Harris, Anne M. Archibald, Antônio H. Ribeiro, Fabian Pedregosa, Paul van Mulbregt, and SciPy 1.0 Contributors. SciPy 1.0: Fundamental Algorithms for Scientific Computing in Python. *Nature Methods*, 17:261–272, 2020.

doi:10.1038/s41592-019-0686-2.

[17] C. K. Law. Interaction between a moving mirror and radiation pressure: A hamiltonian formulation. *Phys. Rev. A*, 51:2537–2541, Mar 1995. doi: 10.1103/PhysRevA.51.2537. URL <https://link.aps.org/doi/10.1103/PhysRevA.51.2537>.

[18] Daniel Malz and Andreas Nunnenkamp. Floquet approach to bichromatically driven cavity-optomechanical systems. *Physical Review A*, 94:023803, Aug 2016. doi: 10.1103/PhysRevA.94.023803. URL <https://link.aps.org/doi/10.1103/PhysRevA.94.023803>.

[19] Daniel Malz and Andreas Nunnenkamp. Optomechanical dual-beam backaction-evading measurement beyond the rotating-wave approximation. *Phys. Rev. A*, 94: 053820, Nov 2016. doi:10.1103/PhysRevA.94.053820. URL <https://link.aps.org/doi/10.1103/PhysRevA.94.053820>.

[20] Daniel Hendrik Malz. Periodic driving and nonreciprocity in cavity optomechanics. PhD thesis, University of Cambridge, 2019. URL <https://www.repository.cam.ac.uk/handle/1810/283253>.

[21] Emma Edwina Wollman. Quantum Squeezing of Motion in a Mechanical Resonator. PhD thesis, California Institute of Technology, 2015.

Appendix A: Solving the noise equation of motions

We start with the equations of motion, where the optics is in a rotating frame and the mechanics in the lab frame.

$$\dot{\hat{d}} = i\Delta\hat{d} + -ig_0(\bar{\alpha}_-e^{i\omega_dt} + \bar{\alpha}_c + \bar{\alpha}_+e^{-i\omega_dt} + \hat{d})(\bar{\beta}_0 + \bar{\beta}_1e^{-i\omega_dt} + \hat{c} + \bar{\beta}_0 + \bar{\beta}_1^*e^{i\omega_dt} + \hat{c}^\dagger) - \frac{\kappa}{2}\hat{d} - \sqrt{\kappa}\hat{d}_{\text{in}} \quad (\text{A1})$$

$$\dot{\hat{c}} = -i\omega_{\text{eff}}(F_2)\hat{c} + ig_0(\bar{\alpha}_-^*e^{-i\omega_dt} + \bar{\alpha}_c^* + \bar{\alpha}_+^*e^{i\omega_dt} + \hat{d}^\dagger)(\bar{\alpha}_-e^{i\omega_dt} + \bar{\alpha}_c + \bar{\alpha}_+e^{-i\omega_dt} + \hat{d}) - \frac{\Gamma}{2}\hat{c} - \sqrt{\Gamma}\hat{c}_{\text{in}} \quad (\text{A2})$$

Linearizing these equations gives

$$\dot{\hat{d}} = i\tilde{\Delta}\hat{d} + ig_0(\bar{\alpha}_-e^{i\omega_dt}\hat{c} + \bar{\alpha}_c\hat{c} + \bar{\alpha}_+e^{-i\omega_dt}\hat{c} + \bar{\alpha}_-e^{i\omega_dt}\hat{c}^\dagger + \bar{\alpha}_c\hat{c}^\dagger + \bar{\alpha}_+e^{-i\omega_dt}\hat{c}^\dagger + \hat{d}\bar{\beta}_1e^{-i\omega_dt} + \hat{d}\bar{\beta}_1^*e^{i\omega_dt}) - \frac{\kappa}{2}\hat{d} - \sqrt{\kappa}\hat{d}_{\text{in}} \quad (\text{A3})$$

$$\dot{\hat{c}} = -i\omega_{\text{eff}}(F_2)\hat{c} + ig_0(\bar{\alpha}_-^*e^{-i\omega_dt}\hat{d} + \bar{\alpha}_c^*\hat{d} + \bar{\alpha}_+^*e^{i\omega_dt}\hat{d} + \bar{\alpha}_-e^{i\omega_dt}\hat{d}^\dagger + \bar{\alpha}_c\hat{d}^\dagger + \bar{\alpha}_+e^{-i\omega_dt}\hat{d}^\dagger) - \frac{\Gamma}{2}\hat{c} - \sqrt{\Gamma}\hat{c}_{\text{in}} \quad (\text{A4})$$

and the conjugate

$$\dot{\hat{d}}^\dagger = -i\tilde{\Delta}\hat{d}^\dagger - ig_0(\bar{\alpha}_-^*e^{-i\omega_dt}\hat{c}^\dagger + \bar{\alpha}_c^*\hat{c}^\dagger + \bar{\alpha}_+^*e^{i\omega_dt}\hat{c}^\dagger + \bar{\alpha}_-e^{-i\omega_dt}\hat{c} + \bar{\alpha}_c^*\hat{c} + \bar{\alpha}_+^*e^{i\omega_dt}\hat{c} + \hat{d}^\dagger\bar{\beta}_1^*e^{i\omega_dt} + \hat{d}^\dagger\bar{\beta}_1e^{-i\omega_dt}) - \frac{\kappa}{2}\hat{d}^\dagger - \sqrt{\kappa}\hat{d}_{\text{in}} \quad (\text{A5})$$

$$\dot{\hat{c}}^\dagger = i\omega_{\text{eff}}(F_2)\hat{c}^\dagger - ig_0(\bar{\alpha}_-e^{i\omega_dt}\hat{d}^\dagger + \bar{\alpha}_c\hat{d}^\dagger + \bar{\alpha}_+e^{-i\omega_dt}\hat{d}^\dagger + \bar{\alpha}_-^*e^{-i\omega_dt}\hat{d} + \bar{\alpha}_c^*\hat{d} + \bar{\alpha}_+^*e^{i\omega_dt}\hat{d}) - \frac{\Gamma}{2}\hat{c}^\dagger - \sqrt{\Gamma}\hat{c}_{\text{in}}^\dagger \quad (\text{A6})$$

where $\tilde{\Delta} = \Delta + g_0(\bar{\beta}_0 + \bar{\beta}_0^*)$. We note that both in the optical equation of motion as well as in the mechanical one there are rotating terms. By going into a rotating frame of the mechanics some of the terms could become stationary. However, without neglecting some of the contributions further analysis is needed. Following [18] the Floquet theory stipulates that we expand the operators in terms of a Fourier components:

$$\hat{d}(t) = \sum_{n=-\infty}^{\infty} e^{in\omega_dt} \hat{d}^{(n)}(t) \quad (\text{A7})$$

$$\hat{d}^\dagger(t) = \sum_{n=-\infty}^{\infty} e^{in\omega_dt} \hat{d}^{(n)\dagger}(t) \quad (\text{A8})$$

$$\hat{c}(t) = \sum_{n=-\infty}^{\infty} e^{in\omega_dt} \hat{c}^{(n)}(t) \quad (\text{A9})$$

$$\hat{c}^\dagger(t) = \sum_{n=-\infty}^{\infty} e^{in\omega_dt} \hat{c}^{(n)\dagger}(t) \quad (\text{A10})$$

and then also define

$$\hat{d}^{(n)}(\omega) = \int_{-\infty}^{\infty} dt e^{i\omega t} \hat{d}^{(n)}(t) \quad (\text{A11})$$

$$\hat{d}^{(n)\dagger}(\omega) = \int_{-\infty}^{\infty} dt e^{i\omega t} \hat{d}^{(n)\dagger}(t) \quad (\text{A12})$$

We note that this convention uses $[\hat{d}^{(n)}(\omega)]^\dagger = \hat{d}^{(-n)\dagger}(-\omega)$. Moving along, when we take the derivative of one of the Fourier components, we must invoke the chain law:

$$\dot{\hat{d}} = \frac{d}{dt} \sum_{n=-\infty}^{\infty} e^{in\omega_d t} \hat{d}^{(n)}(t) = (in\omega_d) \sum_{n=-\infty}^{\infty} e^{in\omega_d t} \hat{d}^{(n)}(t) + \sum_{n=-\infty}^{\infty} e^{in\omega_d t} \dot{\hat{d}}^{(n)}(t) \quad (\text{A13})$$

We now insert these expressions into the equations of motion to find

$$\begin{aligned} \sum_{n=-\infty}^{\infty} e^{in\omega_d t} \dot{\hat{d}}^{(n)}(t) &= \sum_{n=-\infty}^{\infty} e^{in\omega_d t} (i\tilde{\Delta} - in\omega_d) \hat{d}^{(n)}(t) + ig_0 \left(\bar{\alpha}_- e^{i\omega_d t} \sum_{n=-\infty}^{\infty} e^{in\omega_d t} \hat{c}^{(n)}(t) + \bar{\alpha}_+ e^{-i\omega_d t} \sum_{n=-\infty}^{\infty} e^{in\omega_d t} \hat{c}^{(n)\dagger}(t) \right) \\ &\quad + ig_0 \left(\bar{\alpha}_- e^{i\omega_d t} \sum_{n=-\infty}^{\infty} e^{in\omega_d t} \hat{c}^{(n)\dagger}(t) + \bar{\alpha}_+ e^{-i\omega_d t} \sum_{n=-\infty}^{\infty} e^{in\omega_d t} \hat{c}^{(n)}(t) \right) \\ &\quad + ig_0 \bar{\alpha}_c \left(\sum_{n=-\infty}^{\infty} e^{in\omega_d t} \hat{c}^{(n)}(t) + \sum_{n=-\infty}^{\infty} e^{in\omega_d t} \hat{c}^{(n)\dagger}(t) \right) \\ &\quad + ig_0 \left(\bar{\beta}_1 e^{-i\omega_d t} \sum_{n=-\infty}^{\infty} e^{in\omega_d t} \hat{d}^{(n)}(t) + \bar{\beta}_1^* e^{i\omega_d t} \sum_{n=-\infty}^{\infty} e^{in\omega_d t} \hat{d}^{(n)}(t) \right) \\ &\quad - \frac{\kappa}{2} \sum_{n=-\infty}^{\infty} e^{in\omega_d t} \hat{d}^{(n)}(t) - \sqrt{\kappa} \sum_{n=-\infty}^{\infty} e^{in\omega_d t} \hat{d}_{\text{in}}^{(n)}(t) \end{aligned} \quad (\text{A14})$$

$$\begin{aligned} \sum_{n=-\infty}^{\infty} e^{in\omega_d t} \dot{\hat{c}}^{(n)}(t) &= \sum_{n=-\infty}^{\infty} e^{in\omega_d t} (-i\omega_{\text{eff}}(F_2) - in\omega_d) \hat{c}^{(n)}(t) - \\ &\quad + ig_0 \left(\bar{\alpha}_- e^{i\omega_d t} \sum_{n=-\infty}^{\infty} e^{in\omega_d t} \hat{d}^{(n)}(t) + \bar{\alpha}_+ e^{-i\omega_d t} \sum_{n=-\infty}^{\infty} e^{in\omega_d t} \hat{d}^{(n)\dagger}(t) \right) \\ &\quad + ig_0 \left(\bar{\alpha}_-^* e^{-i\omega_d t} \sum_{n=-\infty}^{\infty} e^{in\omega_d t} \hat{d}^{(n)}(t) + \bar{\alpha}_+^* e^{i\omega_d t} \sum_{n=-\infty}^{\infty} e^{in\omega_d t} \hat{d}^{(n)\dagger}(t) \right) \\ &\quad + ig_0 \left(\bar{\alpha}_c^* \sum_{n=-\infty}^{\infty} e^{in\omega_d t} \hat{d}^{(n)}(t) + \bar{\alpha}_c \sum_{n=-\infty}^{\infty} e^{in\omega_d t} \hat{d}^{(n)\dagger}(t) \right) - \frac{\Gamma}{2} \sum_{n=-\infty}^{\infty} e^{in\omega_d t} \hat{c}^{(n)}(t) \end{aligned} \quad (\text{A15})$$

$$\begin{aligned} -\sqrt{\Gamma} \sum_{n=-\infty}^{\infty} e^{in\omega_d t} \hat{c}_{\text{in}}^{(n)}(t). \end{aligned} \quad (\text{A15})$$

If we multiply in the rotating terms into the sums and then shift the indices we can remove the sums such that

$$\begin{aligned} \dot{\hat{d}}^{(n)} &= (i\tilde{\Delta} - in\omega_d) \hat{d}^{(n)} + ig_0 \left(\bar{\alpha}_- \hat{c}^{(n-1)} + \bar{\alpha}_+ \hat{c}^{(n+1)\dagger} \right) + ig_0 \left(\bar{\alpha}_- \hat{c}^{(n-1)\dagger} + \bar{\alpha}_+ \hat{c}^{(n+1)} \right) + ig_0 \bar{\alpha}_c \left(\hat{c}^{(n)} + \hat{c}^{(n)\dagger} \right) \\ &\quad + ig_0 \left(\bar{\beta}_1 \hat{d}^{(n+1)} + \bar{\beta}_1^* \hat{d}^{(n-1)} \right) - \frac{\kappa}{2} \hat{d}^{(n)} - \sqrt{\kappa} \hat{d}_{\text{in}}^{(n)} \\ \dot{\hat{c}}^{(n)} &= (-i\omega_{\text{eff}}(F_2) - in\omega_d) \hat{c}^{(n)} + ig_0 \left(\bar{\alpha}_- \hat{d}^{(n-1)\dagger} + \bar{\alpha}_+ \hat{d}^{(n+1)\dagger} \right) + ig_0 \left(\bar{\alpha}_-^* \hat{d}^{(n+1)} + \bar{\alpha}_+^* \hat{d}^{(n-1)} \right) + ig_0 \left(\bar{\alpha}_c^* \hat{d}^{(n)} + \bar{\alpha}_c \hat{d}^{(n)\dagger} \right) \\ &\quad - \frac{\Gamma}{2} \hat{c}^{(n)} - \sqrt{\Gamma} \hat{c}_{\text{in}}^{(n)}. \end{aligned} \quad (\text{A16})$$

The equivalent conjugate equations are

$$\begin{aligned}\dot{\hat{d}}^{(n)\dagger} &= \left(-i\tilde{\Delta} - in\omega_d\right)\hat{d}^{(n)\dagger} - ig_0\left(\bar{\alpha}_-^*\hat{c}^{(n+1)\dagger} + \bar{\alpha}_+^*\hat{c}^{(n-1)\dagger}\right) - ig_0\left(\bar{\alpha}_-^*\hat{c}^{(n+1)} + \bar{\alpha}_+^*\hat{c}^{(n-1)\dagger}\right) \\ &\quad - ig_0\bar{\alpha}_c^*\left(\hat{c}^{(n)\dagger} + \hat{c}^{(n)}\right) - ig_0\left(\bar{\beta}_1^*\hat{d}^{(n-1)\dagger} + \bar{\beta}_1\hat{d}^{(n+1)\dagger}\right) - \frac{\kappa}{2}\hat{d}^{(n)\dagger} - \sqrt{\kappa}\hat{d}_{\text{in}}^{(n)\dagger} \\ \dot{\hat{c}}^{(n)\dagger} &= (i\omega_{\text{eff}}(F_2) - in\omega_d)\hat{c}^{(n)\dagger} - ig_0\left(\bar{\alpha}_-^*\hat{d}^{(n+1)} + \bar{\alpha}_+^*\hat{d}^{(n-1)}\right) - ig_0\left(\bar{\alpha}_-^*\hat{d}^{(n-1)\dagger} + \bar{\alpha}_+^*\hat{d}^{(n+1)\dagger}\right) - ig_0\left(\bar{\alpha}_c\hat{d}^{(n)\dagger} + \bar{\alpha}_c^*\hat{d}^{(n)}\right) \\ &\quad - \frac{\Gamma}{2}\hat{c}^{(n)\dagger} - \sqrt{\Gamma}\hat{c}_{\text{in}}^{(n)\dagger}.\end{aligned}\quad (\text{A17})$$

Casting this into a matrix equation we get

$$\begin{pmatrix} i(\omega + \omega_d) + A^{(0)} & A^{(-1)} & 0 & 0 \\ A^{(1)} & i\omega + A^{(0)} & A^{(-1)} & 0 \\ 0 & A^{(1)} & i(\omega - \omega_d) + A^{(0)} & 0 \\ 0 & 0 & 0 & 0 \end{pmatrix} \times \begin{pmatrix} \hat{\mathbf{x}}^{(-1)} \\ \hat{\mathbf{x}}^{(0)} \\ \hat{\mathbf{x}}^{(1)} \\ \hat{\mathbf{x}}_{\text{in}} \end{pmatrix} = \begin{pmatrix} 0 \\ 0 \\ 0 \\ 0 \end{pmatrix} \quad (\text{A18})$$

where

$$A^{(0)} = \begin{pmatrix} -i\tilde{\Delta} + \frac{\kappa}{2} & -ig_0\bar{\alpha}_c & 0 & -ig_0\bar{\alpha}_c \\ -ig_0\bar{\alpha}_c^* & i\omega_{\text{eff}} + \frac{\Gamma}{2} & -ig_0\bar{\alpha}_c & 0 \\ 0 & ig_0\bar{\alpha}_c^* & i\tilde{\Delta} + \frac{\kappa}{2} & ig_0\bar{\alpha}_c^* \\ ig_0\bar{\alpha}_c^* & 0 & ig_0\bar{\alpha}_c & -i\omega_{\text{eff}} + \frac{\Gamma}{2} \end{pmatrix} \quad (\text{A19})$$

and

$$A^{(-1)} = -ig_0 \begin{pmatrix} \bar{\beta}_1 & \bar{\alpha}_+ & 0 & \bar{\alpha}_+ \\ \bar{\alpha}_-^* & 0 & \bar{\alpha}_+ & 0 \\ 0 & -\bar{\alpha}_-^* & -\bar{\beta}_1 & -\bar{\alpha}_-^* \\ -\bar{\alpha}_-^* & 0 & -\bar{\alpha}_+ & 0 \end{pmatrix} \quad (\text{A20})$$

$$A^{(1)} = -ig_0 \begin{pmatrix} \bar{\beta}_1^* & \bar{\alpha}_- & 0 & \bar{\alpha}_- \\ \bar{\alpha}_+^* & 0 & \bar{\alpha}_- & 0 \\ 0 & -\bar{\alpha}_+^* & -\bar{\beta}_1^* & -\bar{\alpha}_+^* \\ -\bar{\alpha}_+^* & 0 & -\bar{\alpha}_- & 0 \end{pmatrix} \quad (\text{A21})$$

and

$$\hat{\mathbf{x}}_{\text{in}} = \left(-\sqrt{\kappa}\hat{d}_{\text{in}} \quad -\sqrt{\Gamma}\hat{d}_{\text{in}} \quad -\sqrt{\kappa}\hat{d}_{\text{in}}^\dagger \quad -\sqrt{\Gamma}\hat{c}_{\text{in}}^\dagger\right)^T. \quad (\text{A22})$$

where we've truncated at $n \pm 2$.

Appendix B: Optical spectrum

The optical equation of motion is

$$\chi_c'^{-1}(\omega)\hat{d}^{(n)} = ig_0(\bar{\alpha}_-^*x^{(n-1)} + \bar{\alpha}_+^*x^{(n+1)} + \bar{\alpha}_c^*x^{(n)}) \quad (\text{B1})$$

and for the conjugate

$$(\chi_c'^{-1})^*(\omega)\hat{d}^{(n)\dagger} = -ig_0(\bar{\alpha}_-^*x^{(n+1)} + \bar{\alpha}_+^*x^{(n-1)} + \bar{\alpha}_c^*x^{(n)}) \quad (\text{B2})$$

To calculate the mechanical contributions to the optical spectrum we return to the time domain and calculate the spectrum of two operators rotating at different frequencies, $\hat{x}_a = \hat{x}(t)e^{ia\omega_d t} = \hat{x}^{(n-a)}(t)$ and $\hat{x}_b = \hat{x}(t)e^{ib\omega_d t} = \hat{x}^{(n-b)}(t)$. In the equation of motion for the optical mode $a, b = -1, 0, 1$. We have

$$\begin{aligned}S_{x_a x_b}(\omega, t) &= \int_{-\infty}^{\infty} d\tau e^{i\omega\tau} \langle \hat{x}(t+\tau)e^{ia\omega_d(t+\tau)}\hat{x}(t)e^{ib\omega_d t} \rangle \\ &= \sum_{n,m} \int_{-\infty}^{\infty} d\tau e^{i\omega\tau} \langle \hat{x}^{(n)}(t+\tau)e^{in\omega_d(t+\tau)}e^{ia\omega_d(t+\tau)}\hat{x}^{(m)}(t)e^{im\omega_d t}e^{ib\omega_d t} \rangle \\ &= \sum_{n,m} e^{i(n+m)\omega_d t} e^{i(a+b)\omega_d t} \int_{-\infty}^{\infty} d\tau e^{i\omega\tau} e^{ia\omega_d\tau} e^{in\omega_d\tau} \langle \hat{x}^{(n)}(t+\tau)\hat{x}^{(m)}(t) \rangle \\ &= \sum_m S_{x_a x_b}^{(m)}(\omega) e^{im\omega_d t}\end{aligned}\quad (\text{B3})$$

If we let $m = m' - n$ we get

$$S_{x_a x_b}(\omega, t) = \sum_{n, m'} e^{im' \omega_d t} e^{i(a+b) \omega_d t} \int_{-\infty}^{\infty} d\tau e^{i\omega\tau} e^{ia\omega_d\tau} e^{in\omega_d\tau} \langle \hat{x}^{(n)}(t+\tau) \hat{x}^{(m'-n)}(t) \rangle \quad (B4)$$

The last integral we can instead write as

$$\int_{-\infty}^{\infty} d\tau e^{i\omega\tau} e^{ia\omega_d\tau} e^{in\omega_d\tau} \langle \hat{x}^{(n)}(t+\tau) \hat{x}^{(m)}(t) \rangle = \int_{-\infty}^{\infty} \frac{d\omega'}{2\pi} \langle \hat{x}^{(n)}(\omega + a\omega_d + n\omega_d) \hat{x}^{(m'-n)}(\omega') \rangle = S_{xx}^{(m')}(\omega + a\omega_d) \quad (B5)$$

We therefore have

$$S_{x_a x_b}(\omega, t) = \sum_m S_{x_a x_b}^{(m)}(\omega) e^{im\omega_d t} = \sum_m e^{im\omega_d t} e^{(a+b)i\omega_d t} S_{xx}^{(m)}(\omega + a\omega_d) \quad (B6)$$

For the steady state spectrum we require that $m = 0$, or $m' = -a - b$. This means that the contribution to the optical spectrum becomes

$$S_{x_a x_b}^{(0)}(\omega) = S_{xx}^{(-a-b)}(\omega + a\omega_d) \quad (B7)$$

This means that the spectrum of the optical mode becomes

$$\begin{aligned} S_{d^\dagger d}^{(0)}(\omega) &= g_0^2 |\chi'_c(\omega)|^2 (|\bar{\alpha}'_-|^2 S_{xx}^{(0)}(\omega + \omega_d) + |\bar{\alpha}'_+|^2 S_{xx}^{(0)}(\omega - \omega_d) + \bar{\alpha}'_- \bar{\alpha}'_+ S_{xx}^{(-2)}(\omega + \omega_d) + \bar{\alpha}'_+ \bar{\alpha}'_- S_{xx}^{(2)}(\omega - \omega_d) + \\ &+ |\bar{\alpha}'_c|^2 S_{xx}^{(0)}(\omega) + \bar{\alpha}'_- \bar{\alpha}'_c S_{xx}^{(-1)}(\omega + \omega_d) + \bar{\alpha}'_+ \bar{\alpha}'_c S_{xx}^{(1)}(\omega - \omega_d) + \bar{\alpha}'_c \bar{\alpha}'_- S_{xx}^{(1)}(\omega) + \bar{\alpha}'_c \bar{\alpha}'_+ S_{xx}^{(-1)}(\omega)) \end{aligned} \quad (B8)$$

where

$$\begin{aligned} S_{xx}^{(m)}(\omega) &= \sum_n \int \frac{d\omega'}{2\pi} \langle \hat{x}^{(n)}(\omega + n\omega_d) \hat{x}^{(m-n)}(\omega') \rangle = \\ &= \sum_n \int \frac{d\omega'}{2\pi} \langle (\hat{c}^{(n)}(\omega + n\omega_d) + \hat{c}^{(n)\dagger}(\omega + n\omega_d)) (\hat{c}^{(m-n)}(\omega') + \hat{c}^{(m-n)\dagger}(\omega')) \rangle \end{aligned} \quad (B9)$$

Appendix C: Mechanical fluctuations

We define the mechanical quadrature as $\hat{X} = \frac{1}{\sqrt{2}} (\hat{c} e^{i\omega_d t + i\theta} + \hat{c}^\dagger e^{-i\omega_d t - i\theta})$. Following the same steps as in Appendix B we get for the mechanical quadrature

$$\begin{aligned} S_{XX}(\omega, t) &= \frac{1}{2} \int_{-\infty}^{\infty} d\tau e^{i\omega\tau} \langle (\hat{c}(t+\tau) e^{i\omega_d(t+\tau)+i\theta} + \hat{c}^\dagger(t+\tau) e^{-i\omega_d(t+\tau)-i\theta}) (\hat{c}(t) e^{i\omega_d t + i\theta} + \hat{c}^\dagger(t) e^{-i\omega_d t - i\theta}) \rangle \\ &= \frac{1}{2} \sum_{n, m} \int_{-\infty}^{\infty} d\tau e^{i\omega\tau} \langle \hat{c}^{(n)}(t+\tau) e^{in\omega_d(t+\tau)} e^{i\omega_d(t+\tau)+i\theta} \hat{c}^{(m)}(t) e^{im\omega_d t} e^{i\omega_d t + i\theta} \rangle \\ &+ \frac{1}{2} \sum_{n, m} \int_{-\infty}^{\infty} d\tau e^{i\omega\tau} \langle \hat{c}^{(n)}(t+\tau) e^{in\omega_d(t+\tau)} e^{i\omega_d(t+\tau)+i\theta} \hat{c}^{(m)\dagger}(t) e^{im\omega_d t} e^{-i\omega_d t - i\theta} \rangle \\ &+ \frac{1}{2} \sum_{n, m} \int_{-\infty}^{\infty} d\tau e^{i\omega\tau} \langle \hat{c}^{(n)\dagger}(t+\tau) e^{in\omega_d(t+\tau)} e^{-i\omega_d(t+\tau)-i\theta} \hat{c}^{(m)}(t) e^{im\omega_d t} e^{i\omega_d t + i\theta} \rangle \\ &+ \frac{1}{2} \sum_{n, m} \int_{-\infty}^{\infty} d\tau e^{i\omega\tau} \langle \hat{c}^{(n)\dagger}(t+\tau) e^{in\omega_d(t+\tau)} e^{-i\omega_d(t+\tau)-i\theta} \hat{c}^{(m)\dagger}(t) e^{im\omega_d t} e^{-i\omega_d t - i\theta} \rangle \end{aligned} \quad (C1)$$

For each term individually we have

$$\begin{aligned} &\sum_{n, m} \int_{-\infty}^{\infty} d\tau e^{i\omega\tau} \langle \hat{c}^{(n)}(t+\tau) e^{in\omega_d(t+\tau)} e^{i\omega_d(t+\tau)+i\theta} \hat{c}^{(m)}(t) e^{im\omega_d t} e^{i\omega_d t + i\theta} \rangle \\ &= \sum_{n, m'} e^{i(n+m)\omega_d t} e^{2i\omega_d t} \int_{-\infty}^{\infty} d\tau e^{i\omega\tau} e^{i\omega_d\tau} e^{in\omega_d\tau} \langle \hat{c}^{(n)}(t+\tau) \hat{c}^{(m)}(t) \rangle e^{2i\theta} \end{aligned} \quad (C2)$$

and

$$\begin{aligned} & \sum_{n,m} \int_{-\infty}^{\infty} d\tau e^{i\omega\tau} \langle \hat{c}^{(n)}(t+\tau) e^{in\omega_d(t+\tau)} e^{i\omega_d(t+\tau)+i\theta} \hat{c}^{(m)\dagger}(t) e^{im\omega_d t} e^{-i\omega_d t-i\theta} \rangle \\ &= \sum_{n,m} e^{i(n+m)\omega_d t} \int_{-\infty}^{\infty} d\tau e^{i\omega\tau} e^{i\omega_d\tau} e^{in\omega_d\tau} \langle \hat{c}^{(n)}(t+\tau) \hat{c}^{(m)\dagger}(t) \rangle \end{aligned} \quad (C3)$$

and

$$\begin{aligned} & \sum_{n,m} \int_{-\infty}^{\infty} d\tau e^{i\omega\tau} \langle \hat{c}^{(n)\dagger}(t+\tau) e^{in\omega_d(t+\tau)} e^{-i\omega_d(t+\tau)-i\theta} \hat{c}^{(m)}(t) e^{im\omega_d t} e^{i\omega_d t+i\theta} \rangle \\ &= \sum_{n,m} e^{i(n+m)\omega_d t} \int_{-\infty}^{\infty} d\tau e^{i\omega\tau} e^{-i\omega_d\tau} e^{in\omega_d\tau} \langle \hat{c}^{(n)\dagger}(t+\tau) \hat{c}^{(m)}(t) \rangle \end{aligned} \quad (C4)$$

and

$$\begin{aligned} & \sum_{n,m} \int_{-\infty}^{\infty} d\tau e^{i\omega\tau} \langle \hat{c}^{(n)\dagger}(t+\tau) e^{in\omega_d(t+\tau)} e^{-i\omega_d(t+\tau)-i\theta} \hat{c}^{(m)\dagger}(t) e^{im\omega_d t} e^{-i\omega_d t-i\theta} \rangle \\ &= \sum_{n,m} e^{i(n+m)\omega_d t} e^{-2i\omega_d t} \int_{-\infty}^{\infty} d\tau e^{i\omega\tau} e^{-i\omega_d\tau} e^{in\omega_d\tau} \langle \hat{c}^{(n)\dagger}(t+\tau) \hat{c}^{(m)\dagger}(t) \rangle e^{-2i\theta}. \end{aligned} \quad (C5)$$

The power spectral density of the quadrature fluctuations will be given by the time-independant contribution for each of the terms above:

$$S_{XX}^{(0)}(\omega) = \frac{1}{2} (S_{cc}^{(-2)}(\omega + \omega_d) e^{2i\theta} + S_{cc^\dagger}^{(0)}(\omega + \omega_d) + S_{c^\dagger c}^{(0)}(\omega - \omega_d) + S_{c^\dagger c^\dagger}^{(2)}(\omega - \omega_d) e^{-2i\theta}) \quad (C6)$$